MODELING, IDENTIFICATION AND CONTROL, 1980, VOL. 1, NO. 4, 195–213

Slow drift oscillations of a ship in irregular waves†

ODD M. FALTINSEN‡ and ARNE E. LØKEN§

Keywords: *Hydrodynamics, slowly varying wave forces, wave drift forces, strip theory, mooring, potential theory.*

A procedure to calculate horizontal slow drift excitation forces on an infinitely long horizontal cylinder in irregular beam sea waves is presented. The hydrodynamic boundary-value problem is solved correctly to second order in wave amplitude. Results in the form of second order transfer functions are presented for different, two-dimensional shapes. It is concluded that Newman's approximative method is a practical way to calculate slow drift excitation forces on a ship in beam sea and it is suggested that it may be used in a more general case. Applications of the results for moored ships are discussed.

1. Introduction

Slow drift oscillations of a moored structure in irregular waves may be an important problem. The large, horizontal excursions that occur can cause large forces in anchor lines and limitations in drilling operations.

Hsu and Blenkarn (1970) have given a simple explanation of the phenomena. They imagine the irregular wave system divided into approximate regular wave parts. In each regular wave part, the structure will experience a constant horizontal driftforce (and yaw moment). This is illustrated in Fig. 1, where the driftforce in each 'regular wave part' is indicated by an arrow. In this way a slowly varying excitation force is obtained. The magnitude is not large but, if the mean period is close to a natural period in yaw, sway or surge, a significant amplification may occur due to small damping in the system.

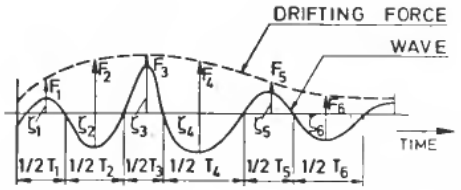

Figure 1. Irregular wave system divided into approximate regular wave parts, showing slowly varying horizontal drift force.

The slow drift excitation forces may also be important for dynamic positioning of offshore structures, manoeuvering of ships in a seaway and analysis of offshore loading. For large volume structures with a small waterplane area, the slow drift excitation forces and moments may create large pitch, roll and heave oscillations.

Received 18th September 1979.

† This paper has been published in Applied Ocean Research, 1979, Vol. 1, No. 1, and is reprinted in MIC with the permission of the authors and the publisher.

‡ Professor at The Norwegian Institute of Technology, Trondheim, Norway.

§ Senior Research Engineer, Det norske Veritas, Høvik, Norway.

The drift force and moment in regular waves is the important building brick in Hsu and Blenkarn's analysis of the slowly varying driftforce and moments. The same is true in the approach by Remery and Hermans (1971) and Newman (1974). A priori they disregard several nonlinear interaction terms between the waves and the structure. In this paper, a new procedure to calculate slow drift excitation forces on an infinitely long horizontal cylinder in irregular beam sea waves is presented. The hydrodynamic boundary value problem is formulated and solved correctly to second order in wave amplitude. The first order problem is the wellknown linear problem commonly used in strip theory calculations of ship motion, and the second order problem contains the necessary slow drift excitation forces. The second order potential satisfied Laplace equation with inhomogeneous boundary condition on the free surface and the body boundary. Green's second identity is used to derive a formula for the drift force and slowly varying horizontal force. All nonlinear interaction terms are included in the theory. The results are presented in the form of second order transfer functions. Some details about theory are found in the next section. The following three sections present numerical results of second order transfer functions for different two-dimensional shapes. The different contributions to the second order transfer functions are examined and the theory is compared to the simplified approach by Newman (1974). In the final section, the application of the results to slow drift oscillations of moored ships is discussed.

2. Theory

Consider an infinitely long horizontal cylinder in longcrested irregular beam sea waves in infinite water depth. A cross-section is shown in Fig. 2. The problem is two-dimensional in the cross-sectional plane and we will choose a coordinate system $(\bar{x}, \bar{y})$ which is fixed, with respect to the structure, and coincides with the inertial system, (x, y), when the structure is at rest. $y=0$ is in the mean free surface and positive y-axis is upwards. The $\bar{y}$-axis is symmetry axis for the structure.

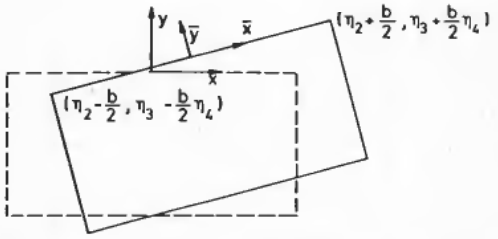

Figure 2. Cross-section of infinitely long horizontal cylinder in long-crested irregular beam sea waves in infinite water depth.

Let us assume the fluid to be incompressible and the fluid motion irrotational so that there exists a velocity potential ϕ which satisfies the Laplace equation

$$\frac{\partial^2\phi}{\partial x^2}+\frac{\partial^2\phi}{\partial y^2}=0 \tag{1}$$

The solution will be written as a series expansion in a parameter δ characterizing the

smallness of the wave amplitudes, i.e. we write

$$\phi=\phi_1+\phi_2+\ \ldots \tag{2}$$

where ϕ_1 is linear with respect to δ, ϕ_2 is quadratic with respect to δ, and so forth.

Let the incident waves propagate along the positive x-axis. The incident wave potential correct to first order in wave amplitude can be written as

$$\phi^{\mathrm{I}}=\sum_{i=1}^{N}\frac{gA_i}{\omega_i}\exp(\nu_i y)\sin(\nu_i x-\omega_i t+\epsilon_i) \tag{3}$$

Here t is the time variable, g the acceleration of gravity, ω_i the circular frequency of oscillation and ν_i the wave number of wave component number i. ω_i and ν_i are connected through the dispersion relationship $\omega_i^2/g=\nu_i$. The phase angles ϵ_i may be considered as random phase angles and the amplitudes A_i of the wave components may be determined by a wave spectrum $S(\omega)$, characterizing the sea state. If the important part of the wave energy is concentrated between the circular frequencies $\omega_{\min}$ and $\omega_{\max}$, we divide the frequency interval $\omega_{\min}$ to $\omega_{\max}$ into N equal subintervals and call the midpoints of the ith interval ω_i. A_i is then determined by

$$\frac{A_i^2}{2}=S(\omega_i)\frac{\omega_{\max}-\omega_{\min}}{N} \tag{4}$$

The limit of the sum (3) when the subintervals go to zero, $\omega_{\min}\to 0$ and $\omega_{\max}\to\infty$, is

$$\phi^{\mathrm{I}}=\int_0^{\infty}\frac{g}{\omega}\exp(\nu y)\cos(\nu x-\omega t+\epsilon(\omega))\sqrt{(2S(\omega)d\omega)} \tag{5}$$

From a practical point of view, eqns. (3) and (5) are the same. Equations (3) or (5) is a first order approximation of the incident wave-field. Note that our solution will contain a second order correction to the incident wave potential that is slowly varying in time and propagates along the positive x-axis.

The problem of selecting appropriate design spectra is a difficult one. Different analytical spectral forms are recommended in the literature. Examples are the Pierson–Moskowitz spectrum, ISSC-spectrum, Scott–Wiegel spectrum and the ITTC-spectrum. The Jonswap spectrum is often used for the North-Sea Offshore operations. Houmb and Overvik (1976) have recommended a practical way to determine the parameters of the Jonswap spectrum, on the basis of a given significant wave height and mean period.

In reality the seaway is not longcrested. Reliable information about shortcrested waves is scarce. The cosinus square directional function is often used. In general, the directional function is frequency-dependent and dependent on the site. In principle, it is possible to generalize our procedure to take into account the shortcrestedness of the waves.

Details about the solution of the first and second order problem are given by Faltinsen and Løken (1978 a). It should be noted that the influence of the first order motions in heave (η_3), sway (η_2) and roll (η_4) are included in the first order potential, ϕ_1, while the effect of second order motions is not included in the second order potential, ϕ_2. This implies that the second order force we discuss below is an excitation force to the second order motion.

The second order slowly varying horizontal excitation force may be obtained through the Bernoulli's equation

$$p=-\rho gy-\rho\frac{\partial\phi}{\partial t}-\frac{\rho}{2}\left[\left(\frac{\partial\phi}{\partial x}\right)^2+\left(\frac{\partial\phi}{\partial y}\right)^2\right]+p_0$$

where p is the fluid pressure and p_0 atmospheric pressure. By Taylor expansion, we can write the pressure on the body, p_s, in terms of the values on the mean position of the body. This is indicated by the index m in the expression below. We can write

$$p_s=-\rho gy-\rho\frac{\partial\phi_1}{\partial t}\bigg|_m-\rho\frac{\partial\phi_2}{\partial t}\bigg|_m-\rho(\eta_2-\bar{y}\eta_4)\frac{\partial^2\phi_1}{\partial t\partial x}\bigg|_m$$
$$-\rho(\eta_3+\bar{x}\eta_4)\frac{\partial^2\phi_1}{\partial t\partial y}\bigg|_m-\frac{\rho}{2}\left[\left(\frac{\partial\phi_1}{\partial x}\right)^2+\left(\frac{\partial\phi_1}{\partial y}\right)^2\right]\bigg|_m+p_0 \quad (6)$$

This is correct to second order in wave amplitude. The first term in (6) is the hydrostatic pressure, which causes the following horizontal force pr. unit length on the body

$$F_2^{HS}=\frac{\rho g}{2}\left\{\left(\frac{1}{g}\frac{\partial\phi_1}{\partial t}\right)^2\bigg|_{\substack{x=b/2\\y=0}}-\left(\frac{1}{g}\frac{\partial\phi_1}{\partial t}\right)^2\bigg|_{\substack{x=-b/2\\y=0}}\right\} \quad (7)$$

where b is the beam at water line.

The second term in eqn. (6) is a first order term. To derive a force-expression correct to second order, we have to be careful about the integration of the pressure term and take proper account of the changing wetted surface of the body. It is possible to show that the second term causes a slowly varying horizontal force pr. unit length, which can be derived from the expression

$$F_2^{\phi_1}=\rho\frac{\partial\phi_1}{\partial t}\bigg|_{\substack{x=b/2\\y=0}}\left\{\left(-\frac{1}{g}\frac{\partial\phi_1}{\partial t}\right)\bigg|_{\substack{x=b/2\\y=0}}-(\eta_3+b/2\eta_4)\right\}$$
$$-\frac{\partial\phi_1}{\partial t}\bigg|_{\substack{x=-b/2\\y=0}}\left\{\left(-\frac{1}{g}\frac{\partial\phi_1}{\partial t}\right)\bigg|_{\substack{x=-b/2\\y=0}}-(\eta_3-b/2\eta_4)\right\}-\eta_4\left(M\frac{d^2\eta_3}{dt^2}+\rho gb\eta_3\right) \quad (8)$$

where M is the mass pr. unit length of the cylinder. An incorrect version of eqn. (8) was presented by Faltinsen and Løken (1978 a), but this did not influence their numerical results.

The slowly varying horizontal force pr. unit length, due to the third term in eqn. (6), has been derived by Faltinsen and Løken (1978 a). The contribution to the slowly varying horizontal force pr. unit length on the rest of the terms in eqn. (6) can be derived from

$$F_2^{Q}=\int_{\bar{S}}\left\{\rho(\eta_2-\bar{y}\eta_4)\frac{\partial^2\phi_1}{\partial t\partial x}\bigg|_m+\rho(\eta_3+\bar{x}\eta_4)\frac{\partial^2\phi_1}{\partial t\partial y}\bigg|_m\right.$$
$$\left.+\frac{\rho}{2}\left[\left(\frac{\partial\phi_1}{\partial x}\right)^2+\left(\frac{\partial\phi_1}{\partial y}\right)^2\right]\bigg|_m\right\}n_2\,ds \quad (9)$$

where n_2 is the horizontal component of the unit normal vector $\boldsymbol{n}$ to the average wetted body surface S per pr. unit length. ($\boldsymbol{n}$ is positive into the fluid).

The horizontal slow drift excitation forces pr. unit length can be written as

$$F_H^{SV} = \sum_{i=1}^{N} \sum_{j=1}^{N} A_i A_j \{T_{ij}^c \cos((\omega_j - \omega_i)t - (\epsilon_j - \epsilon_i)) + T_{ij}^s \sin((\omega_j - \omega_i)t - (\epsilon_j - \epsilon_i))\} \quad (10)$$

The mean drift force pr. unit length is easily obtained from (10) as

$$\overline{F_H^{SV}} = \sum_{i=1}^{N} A_i^2 T_{ii}^c \quad (11)$$

T_{ij}^c and T_{ij}^s are independent of A_i, A_j, ϵ_i and ϵ_{j_2} and can be considered as second order transfer functions. $A_i^2\ T_{ii}^c$ is the drift force in regular sinusoidal waves of circular frequency ω_i and wave amplitude A_i.

A degree of ambiguity exists in the coefficients T_{ij}^c and T_{ij}^s when $i \neq j$. We could, for example, impose the restriction that T_{ij}^c and T_{ij}^s are equal to zero when $i > j$. Another possibility is to require that $T_{ij}^c = T_{ji}^c$ and $T_{ij}^s = -T_{ji}^s$ when $j \neq i$. This definition was followed by Newman (3) and, in presentation of our results, we will follow the same procedure. It should be noted that Newman's simplifying approach was to assume that $T_{ij}^c = T_{ii}^c$ and $T_{ij}^s = 0$ in eqn. (10).

Equation (10) can be written as an integral formulation in the same way as eqn. (3) was written as eqn. (5). We can write

$$F_H^{SV} = \int_0^\infty \int_0^\infty \{T^c(\omega, \omega') \cos((\omega - \omega')t - (\epsilon(\omega) - \epsilon(\omega')) + T^s(\omega, \omega') \sin((\omega - \omega')t - (\epsilon(\omega) - \epsilon(\omega'))\} \cdot \sqrt{4S(\omega)S(\omega')}\, d\omega\, d\omega' \quad (12)$$

The mean drift force can be written as

$$\overline{F_H^{SV}} = \int_0^\infty 2S(\omega) T^c(\omega, \omega)\, d\omega \quad (13)$$

3. Numerical results

The method described in the last chapter has been used to calculate second order transfer functions and slowly varying horizontal exciting force on infinitely long horizontal cylinders in irregular, longcrested beam sea waves. Four different sectional shapes were used. The main particulars are given in Table 1. $\overline{GM}$ is the transverse metacentric height, RRG the roll radius of gyration with respect to an axis in water plane right above centre of gravity, Y_a is the vertical coordinate of the centre of gravity, b is the beam at waterline and d is the sectional draft.

Shape	$\frac{\overline{GM}}{b}$	$\frac{RRG}{b}$	$\frac{Y_a}{b}$
Circular Cylinder $b/d = 2{\cdot}0$	0·127	0·26	−0·125
Rectangular Cylinder $b/d = 2{\cdot}0$	0·042	0·25	−0·125
Rectangular Cylinder $b/d = \frac{20}{7}$	0·139	0·25	−0·125
Rectangular Cylinder $b/d = \frac{20}{15}$	0·188	0·25	−0·125

Table 1.

We did not have experimental results to compare our numerical results with. Model tests are difficult to perform because of the small quantities we are dealing with. There are different ways we could do the model tests. One way is to conduct tests with two simultaneous regular wave trains of circular frequencies ω_i and ω_j incident on a long cylinder orthogonal to the wave propagation direction. The model can be kept in an average position by a system of soft springs. In this way, they do not influence the first order motions significantly.

The slow drift excitation force

$$(T_{ij}^{c}+T_{ji}^{c})\cos((\omega_j-\omega_i)t-(\epsilon_j-\epsilon_i))+(T_{ij}^{s}-T_{ji}^{s})\sin((\omega_j-\omega_i)t-(\epsilon_j-\epsilon_i))$$

can be obtained by measuring the sway response and separating the sway response that is oscillating with circular frequency $\omega_j-\omega_i$. Assuming the low frequency added mass and the spring characteristics to be known, we may use a simple mass-spring mathematical description to obtain the slow drift excitation force. If $\omega_j-\omega_i$ is close to the natural circular frequency in sway for the system, we need to know the damping of the system, which might be difficult to estimate. But the resonance problem can be avoided by changing the spring characteristics. The second order transfer functions can be obtained from the equation above and the symmetry relationships of T_{ij} and T_{ij}^{s}.

Another way to do the model tests would be to simulate irregular waves and obtain the second order transfer function through higher order spectra. The tests would require a long testing period compared with conventional, first order response analysis.

It may be easier to obtain good accuracy by numerical calculations than by model tests. But we would like to point out some of the inaccuracies that are in the numerical calculations. It is then necessary to describe, in some detail, the calculation procedure.

The first order potential is calculated by Lewis form technique, where the velocity potential is written either as a wave source or as a wave dipole (depending on the symmetry of the problem) plus an infinite sum of wave free potentials. The strengths of the source (or the dipole) and the wave free potentials are determined by the body boundary conditions. In the numerical calculation procedure, the infinite sum of wave free potentials is truncated and the body boundary conditions are satisfied for a finite number of points. The number of wave free potential terms in our calculations was six and the number of points where the body boundary condition was satisfied was ten. The body boundary condition was satisfied by setting up a least square condition. The increase of wave free potential terms and points, where the boundary conditions are satisfied, will not increase significantly the accuracy of the first order terms. The influence on the second order transfer functions will be more important. For instance, expression (9) is calculated by evaluating the integrand at the same points where the body boundary conditions are satisfied and then using a simple numerical integration scheme. When the wave lengths are small, the first order variables are changing rapidly in the free surface zone. Therefore, the numer of points on the body boundary we are using in our calculations might be too few in the low wave length range.

In the calculation of the second order transfer function, we need expressions for the first order velocities. This was done by both numerical differentiating and by differentiating the analytical first order expressions. We found a difference of up to 10% on the second order transfer functions by using different differentiation techniques. By comparison with other methods of predicting drift force, we could not say that one differentiation technique was better than another. A better agreement would have

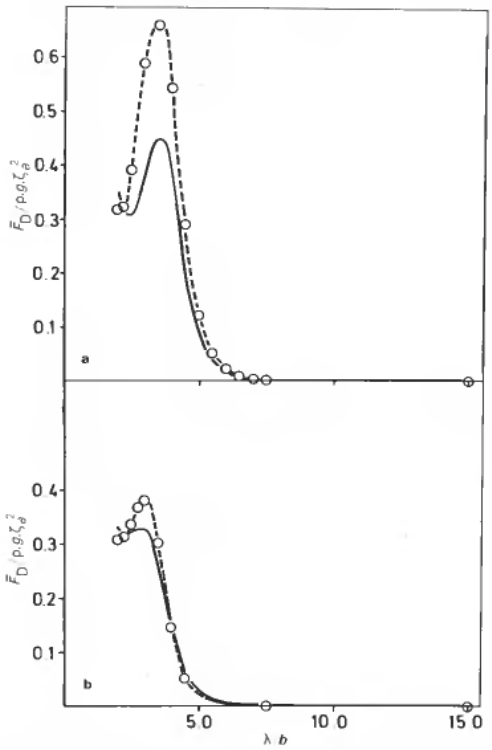

Figure 3. Drift force on (*a*) rectangular box ($b/d = 20/7$) and (*b*) circular cylinder ($b/d = 2$). ———, Maruo; ○———○, Faltinsen.

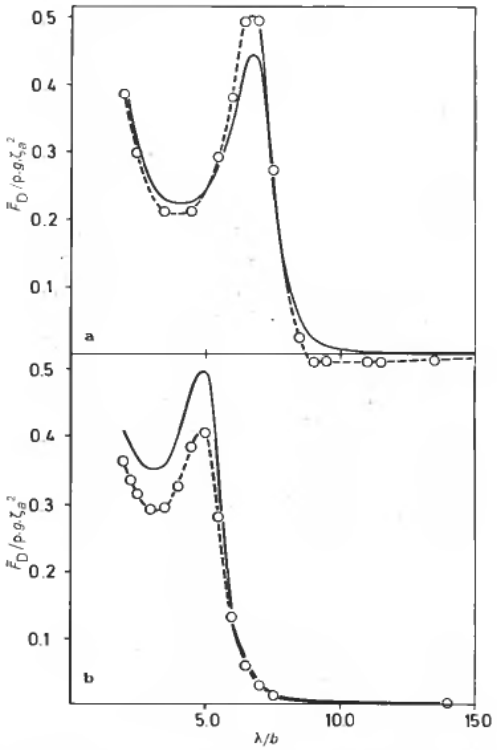

Figure 4. Drift force on (*a*) rectangular box ($b/d = 20/15$) and (*b*) rectangular box ($b/d = 2$). ———, Maruo; ○———○, Faltinsen.

been achieved by increasing the number of wave free potential terms. In the calculations presented here, we obtained velocities by differentiating the analytical expressions.

The calculation of the driftforce in regular waves i.e. the diagonal term T_{ii}^c has been compared with the method of Maruo (1960) which states that the driftforce pr. unit length on an infinitely long horizontal cylinder, in regular beam sea waves, is

$$\bar{F}_D = \frac{\rho g}{2} |A^-|^2$$

where $|A^-|$ is the reflected wave amplitude. We have used Lewis form technique to calculate $|A^-|$ (Faltinsen 1975). In general, the agreement between the two methods is quite good (see Figs. 3 and 4). There are exceptions, however. Better agreement in the low wave length range may have been obtained by increasing the number of points on the body boundary where the boundary condition is satisfied. But the main reason for the discrepancy for the rectangular box ($b/d = 20/7$) is thought to be viscous effects. This is the only cylinder where a large resonance oscillation in roll occurs in the frequency range of interest. The resonance roll occurs at the same wave length where the driftforce has a maximum, i.e. when $\lambda/b \sim 3{\cdot}5$. In the calculation of roll, a viscous roll damping is included. This is a significant term at roll resonance. Maruo's formula is based on potential theory and derived using conservation of energy. He does not take into account any viscous loss. We could therefore not expect good agreement between Maruo's method and our method at roll resonance. For frequencies that are not in the vicinity of roll resonance viscous roll damping will have small effect on the results. The peaks in the driftforce for the other cylinders are due to heave resonance oscillation, where no viscous effects are taken into account. The heave resonance oscillation for the rectangular box ($b/d = 20/15$) is very significant. Its amplitude is 2·7 times the incident wave amplitude. But we note quite good agreement between the two methods.

The second order transfer functions T_{ij}^c and T_{ij}^s (see eqn. (10)) are presented in non-dimensionalized form as functions of $\omega_i\sqrt{(d/g)}$ and $\omega_j\sqrt{(d/g)}$ in Tables 2–9. T_{ij}^c and T_{ij}^s are understood to be two-dimensional values, i.e. values pr. unit length of the cylinder. From the tables, we note that T_{ij}^c and T_{ij}^s are, in general, not changing rapidly when ω_i is close to ω_j. There are some few exceptions which seem to occur in the frequency range where the drift force is changing rapidly, for instance, in the vicinity of a natural frequency of roll.

The second order transfer functions T_{ij}^c and T_{ij}^s, in Tables 2–9, were used together with eqn. (10) to simulate horizontal slow drift excitation force pr. unit length on infinitely long horizontal cylinders in irregular beam sea waves (see Figs. 5–8).

An ISSC-spectrum with zero-upcrossing period $T_z = 5{\cdot}5$ sec and significant wave height $H_s = 2$ m was used to calculate the wave amplitude components A_i. Only 11–14 wave components were used. In a practical case, one may need five times as many components. This is further discussed in the next chapter. All the cylinders had a beam equal to 20 m.

Newman's approach was also used in the calculations. That means T_{ij}^c were set equal to T_{ii}^c and T_{ij}^s were set equal to zero in eqn. (10). Both the present method and Maruo's method were used to evaluate T_{ii}^c. These methods are called Newman–Faltinsen method and Newman–Maruo method, respectively. Simulation by using the complete eqn. (10) is called 'Complete expression' in the figures. Further 'Cosine expression' means that only the cosine part of eqn. (10) is used. We note that the

$\omega_i\sqrt{(d/g)}$ ↓ \ $\omega_j\sqrt{(d/g)}$ →	1·25	1·18	1·12	1·06	0·95	0·89	0·84	0·65
1·25	0·308	0·285	0·259	0·250	0·250	0·240	0·233	0·256
1·18	0·285	0·314	0·306	0·292	0·277	0·246	0·234	0·254
1·12	0·239	0·308	0·338	0·340	0·324	0·267	0·234	0·247
1·06	0·250	0·292	0·340	0·368	0·367	0·301	0·245	0·243
0·95	0·250	0·277	0·324	0·367	0·383	0·329	0·257	0·241
0·89	0·240	0·246	0·267	0·301	0·329	0·303	0·227	0·195
0·84	0·233	0·234	0·234	0·245	0·257	0·227	0·147	0·105
0·65	0·256	0·234	0·247	0·243	0·241	0·195	0·105	0·051

Table 2. Numerical calculations of $T_{ij}{}^{c}/(\rho \cdot g)$ for a circular cylinder in beam sea ($b/d=2{\cdot}0$).

$\omega_i\sqrt{(d/g)}$ ↓ \ $\omega_j\sqrt{(d/g)}$ →	1·25	1·18	1·12	1·06	0·95	0·89	0·84	0·65
1·25	0·0	0·043	0·059	0·061	0·059	0·069	0·112	0·160
1·18	−0·043	0·0	0·030	0·038	0·032	0·028	0·066	0·112
1·12	−0·059	−0·030	0·0	0·015	0·013	0·004	0·041	0·087
1·06	−0·061	−0·038	−0·015	0·0	0·0	−0·006	0·033	0·082
0·95	−0·059	−0·032	−0·013	0·0	0·0	−0·004	0·040	0·094
0·89	−0·069	−0·028	−0·004	0·006	0·004	0·0	0·056	0·129
0·84	−0·11	−0·066	−0·041	−0·033	−0·04	−0·056	0·0	0·09
0·65	−0·160	−0·112	−0·087	−0·082	−0·094	−0·129	−0·09	0·0

Table 3. Numerical calculations of $T_{ij}{}^{s}/(\rho \cdot g)$ for a circular cylinder in beam sea ($b/d=2{\cdot}0$).

$\omega_i\sqrt{(d/g)}$ ↓ / $\omega_j\sqrt{(d/g)}$ →	1·25	1·18	1·12	0·89	0·84	0·79	0·76	0·69
1·25	0·363	0·317	0·272	0·270	0·286	0·302	0·330	0·406
1·18	0·317	0·336	0·305	0·260	0·269	0·264	0·261	0·321
1·12	0·272	0·305	0·315	0·245	0·255	0·248	0·228	0·258
0·89	0·270	0·260	0·245	0·326	0·339	0·313	0·236	0·172
0·84	0·286	0·269	0·255	0·339	0·384	0·380	0·300	0·208
0·79	0·302	0·264	0·248	0·313	0·380	0·405	0·337	0·234
0·76	0·330	0·261	0·228	0·236	0·300	0·337	0·280	0·175
0·69	0·406	0·321	0·258	0·172	0·208	0·234	0·175	0·059

Table 4. Numerical calculations of $T_{ij}^c/(\rho \cdot g)$ for a rectangular cylinder in beam sea ($b/d=2{\cdot}0$)

$\omega_i\sqrt{(d/g)}$ ↓ / $\omega_j\sqrt{(d/g)}$ →	1·25	1·18	1·12	0·89	0·84	0·79	0·76	0·69
1·25	0·0	0·045	0·059	0·050	0·034	0·031	0·049	0·075
1·18	−0·045	0·00	0·034	0·024	0·002	−0·021	−0·014	0·009
1·12	−0·059	−0·034	0·0	0·009	−0·017	−0·047	−0·048	−0·021
0·89	−0·050	−0·024	−0·009	0·0	−0·026	−0·086	−0·115	−0·067
0·84	−0·034	−0·001	0·017	0·026	0·0	−0·068	−0·111	−0·052
0·79	−0·031	0·021	0·047	0·086	0·068	0·0	−0·053	0·008
0·76	−0·049	0·014	0·048	0·113	0·111	0·053	0·0	0·068
0·69	−0·075	−0·009	0·021	0·067	0·052	−0·008	−0·068	0·0

Table 5. Numerical calculations of $T_{ij}^s/(\rho \cdot g)$ for a rectangular cylinder in beam sea ($b/d=2{\cdot}0$)

$\omega_i\sqrt{(d/g)}$ ↓ \ $\omega_j\sqrt{(d/g)}$ →	1·05	0·99	0·94	0·74	0·70	0·66	0·63	0·61
1·05	0·320	0·299	0·291	0·252	0·189	0·190	0·219	0·249
0·99	0·299	0·324	0·340	0·248	0·160	0·148	0·172	0·202
0·94	0·291	0·340	0·392	0·294	0·173	0·140	0·1533	0·178
0·74	0·252	0·248	0·294	0·544	0·406	0·311	0·268	0·250
0·70	0·189	0·160	0·173	0·406	0·290	0·204	0·166	0·150
0·66	0·191	0·148	0·140	0·311	0·204	0·123	0·088	0·073
0·63	0·219	0·172	0·153	0·268	0·166	0·088	0·052	0·038
0·61	0·249	0·202	0·178	0·25	0·150	0·073	0·038	0·023

Table 6. Numerical calculations of $T_{ij}^{c}/(\rho \cdot g)$ for a rectangular cylinder in beam sea ($b/d = 20/7$).

$\omega_i\sqrt{(d/g)}$ ↓ \ $\omega_j\sqrt{(d/g)}$ →	1·05	0·99	0·94	0·74	0·70	0·66	0·63	0·61
1·05	0·0	0·048	0·069	−0·071	−0·025	0·038	0·080	0·105
0·99	−0·048	0·0	0·032	−0·018	−0·125	−0·051	−0·001	0·028
0·94	−0·069	−0·032	0·0	−0·260	−0·221	−0·138	−0·079	−0·043
0·74	0·071	0·175	0·260	0·0	−0·042	0·0	0·044	0·073
0·70	0·025	0·126	0·221	0·042	0·0	0·042	0·089	0·120
0·66	−0·038	0·051	0·138	0·0	−0·042	0·0	0·051	0·088
0·63	−0·080	0·001	0·079	−0·044	−0·089	−0·051	0·0	0·039
0·61	−0·105	−0·028	0·043	−0·073	−0·120	−0·088	−0·039	0·0

Table 7. Numerical calculations of $T_{ij}^{s}/(\rho \cdot g)$ for a rectangular cylinder in beam sea ($b/d = 20/7$).

$\omega_i\sqrt{(d/g)}$ \ $\omega_j\sqrt{(d/g)}$	1·53	1·37	0·97	0·93	0·87	0·85	0·79	0·74
1·53	0·387	0·231	0·323	0·400	0·442	0·455	0·470	0·505
1·37	0·231	0·300	0·178	0·199	0·223	0·239	0·299	0·39
0·97	0·323	0·178	0·240	0·257	0·272	0·277	0·137	0·087
0·93	0·397	0·199	0·257	0·293	0·326	0·348	0·192	0·117
0·87	0·442	0·223	0·272	0·326	0·380	0·424	0·270	0·173
0·85	0·455	0·239	0·277	0·348	0·424	0·493	0·361	0·252
0·79	0·470	0·300	0·137	0·192	0·270	0·361	0·273	0·160
0·74	0·505	0·389	0·088	0·117	0·173	0·252	0·160	0·025

Table 8. Numerical calculations of $T_{ij}^c/(\rho \cdot g)$ for a rectangular cylinder in beam sea ($b/d = 20/15$)

$\omega_i\sqrt{(d/g)}$ \ $\omega_j\sqrt{(d/g)}$	1·53	1·37	0·97	0·93	0·87	0·85	0·79	0·74
1·53	0·0	0·085	0·007	−0·008	−0·022	−0·026	0·027	0·036
1·37	−0·085	0·0	0·027	−0·015	−0·062	−0·101	−0·103	−0·137
0·97	−0·007	−0·027	0·0	0·0	−0·024	−0·083	−0·181	−0·13
0·93	0·008	0·015	0·0	0·0	−0·021	−0·085	−0·209	−0·141
0·87	0·022	0·062	0·024	0·021	0·0	−0·067	−0·223	−0·145
0·85	0·026	0·107	0·083	0·084	0·067	0·0	−0·183	−0·105
0·79	−0·027	0·103	0·181	0·204	0·223	0·183	0·0	0·094
0·74	−0·036	0·137	0·130	0·141	0·145	0·105	−0·094	0·0

Table 9. Numerical calculations of $T_{ij}^s/(\rho \cdot g)$ for a rectangular cylinder in beam sea ($b/d = 20/15$)

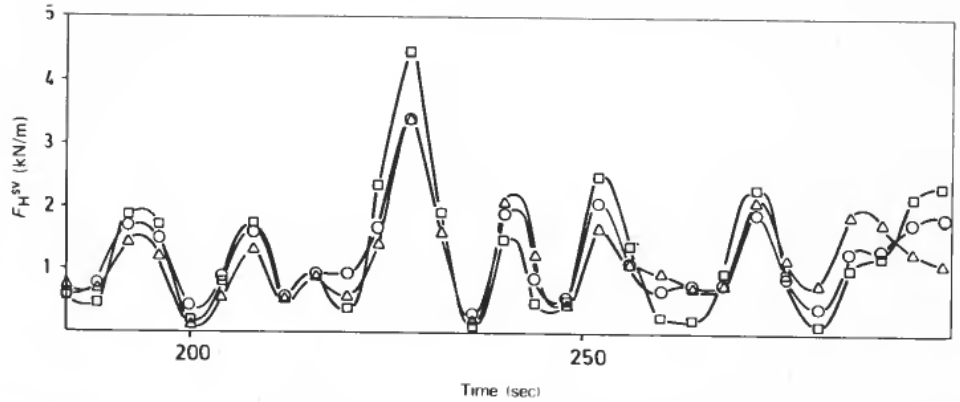

Figure 5. Slowly varying horizontal force per unit length of rectangular cylinder (b/d= 20/15). □, Newman/Faltinsen; △, complete expression; ○, cosine expression.

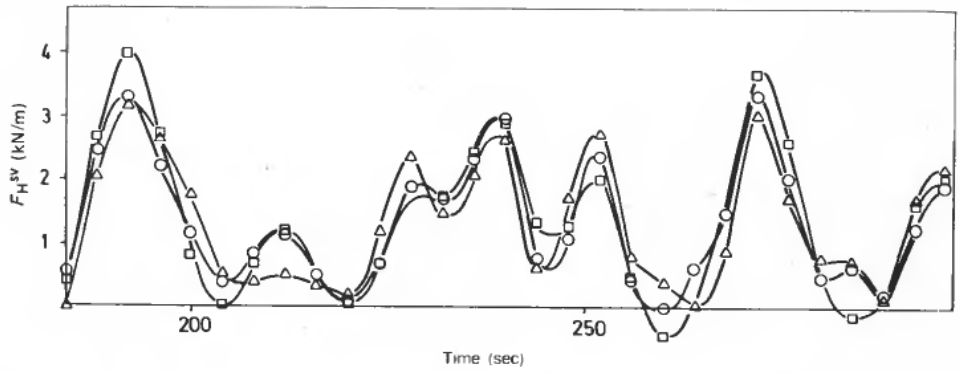

Figure 6. Slowly varying horizontal force per unit length of rectangular cylinder (b/d= 20/7). □, Newman/Faltinsen; △, complete expression; ○, cosine expression.

differences between the different methods are within 20% in the estimation of force amplitudes and the deviation in the characteristic period is small.

The results seem to generally confirm Newman's hypothesis (Newman 1974). This is an important observation having great practical consequences. The evaluation of the second order slowly varying excitation force by Newman's method becomes quite simple, compared with the more exact method presented in this paper. The computer time by our method may be quite large. It took 11 minutes CPU on UNIVAC 1110 to calculate 14 times 14 values of the second order transfer functions T_{ij}^c and T_{ij}^s for three sections.

The importance of the different term in the expression for the slowly varying excitation term has been studied. The results for a rectangular cylinder with $b/d=2$ are presented in Table 10. Each main matrix element is divided into three lines.

The first line is the contribution from the velocity square term in Bernoulli's equation, i.e. the contribution from the last term of eqn. (9)

The second line is the contribution from the second order potential, i.e. the force due to the pressure part

$$-\rho \frac{\partial \phi_2}{\partial t}\bigg|_m$$

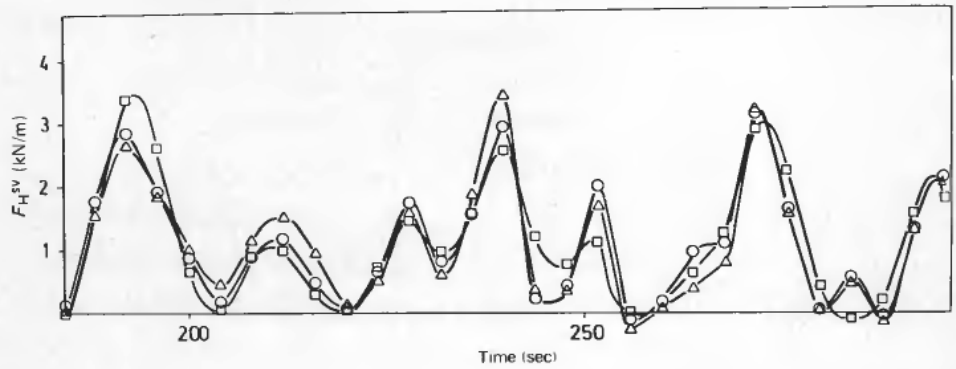

Figure 7. Slowly varying horizontal force per unit length of rectangular box ($b/d=2$). □, Newman/Faltinsen; △, complete expression; ○, cosine expression.

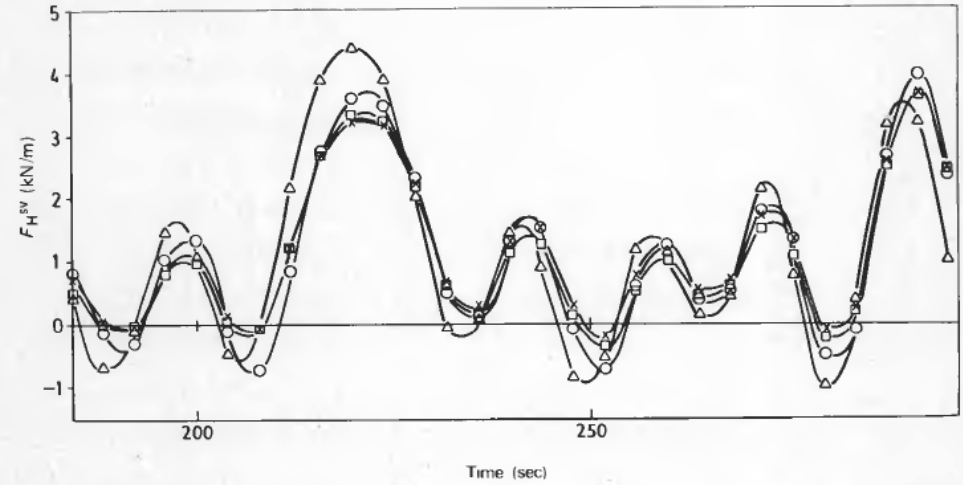

Figure 8. Slowly varying horizontal force per unit length of circular cylinder ($b/d=2$). □, Newman/Faltinsen; ×, Newman/Maruo; △, complete expression; ○, cosine expression.

The last line is the total value of T_{ij}^c. All the numbers are non-dimensionalized by ρg. We note from the table that the velocity square term in Bernoulli's equation gives a completely wrong estimate of T_{ij}^c. This result should be noted, since the velocity square term of Bernoulli's equation is sometimes used to calculate the drift force.

We also note the small influence from the second order potential when ω_i is close to ω_j. When ω_i is not close to ω_j, which is uninteresting in the prediction of slow drift excitation forces, we note that the contribution from the second order potential is important.

4. Applications to moored ships

The numerical results of chapter 3 suggest that the horizontal slow drift excitation force on a ship in irregular beam sea waves can be calculated as

$$F_H^{SV} = \sum_{i=1}^{N} \sum_{j=1}^{N} A_i A_j T_{ii}^c \cos((\omega_j - \omega_i)t - (\epsilon_j - \epsilon_i)) \tag{14}$$

$\omega_i\sqrt{(d/g)}$ ↓	$\omega_j\sqrt{(d/g)}$ → 1·25	1·18	1·12	0·89	0·84	0·79	0·76	0·69
1·25	−0·592 0·0 0·363	−0·580 −0·029 0·317	−0·562 −0·058 0·272	−0·523 −0·018 0·270	−0·586 −0·008 0·286	−0·634 0·040 0·302	−0·513 0·176 0·330	−0·214 0·377 0·406
1·18	−0·580 −0·029 0·317	−0·582 0·0 0·336	−0·573 −0·019 0·305	−0·561 −0·034 0·260	−0·622 −0·028 0·259	−0·659 0·003 0·264	−0·522 0·106 0·261	−0·221 0·289 0·321
1·12	−0·562 −0·058 0·272	−0·573 −0·019 0·305	−0·572 0·0 0·315	−0·588 −0·052 0·245	−0·640 −0·046 0·255	−0·669 −0·021 0·248	−0·522 0·059 0·228	−0·225 0·205 0·258
0·89	−0·523 −0·018 0·270	−0·561 −0·034 0·260	−0·580 −0·052 0·245	−0·630 0·0 0·326	−0·679 −0·012 0·339	−0·687 −0·036 0·313	−0·541 −0·037 0·236	−0·372 0·008 0·172
0·84	−0·586 −0·08 0·286	−0·622 −0·028 0·269	−0·640 −0·046 0·255	−0·679 −0·012 0·339	−0·721 0·0 0·384	−0·725 −0·01 0·380	−0·584 −0·019 0·300	−0·332 −0·002 0·208
0·79	−0·634 −0·040 0·302	−0·659 0·003 0·264	−0·669 −0·021 0·248	−0·687 −0·036 0·313	−0·725 −0·01 0·350	−0·728 0·0 0·405	−0·595 −0·004 0·332	−0·357 0·001 0·234
0·76	−0·513 0·176 0·330	−0·522 0·106 0·261	−0·522 0·059 0·228	−0·541 −0·037 0·236	−0·584 −0·019 0·300	−0·595 −0·004 0·337	−0·477 0·0 0·280	−0·266 0·028 0·175
0·69	−0·214 0·377 0·406	−0·221 0·289 0·321	−0·225 0·205 0·258	−0·281 0·008 0·172	−0·332 −0·003 0·208	−0·357 0·001 0·234	−0·266 0·003 0·175	−0·095 0·0 0·059

Table 10. Numerical calculations of the different main contribution to $T_{ij}^c/(\rho \cdot g)$ for the rectangular cylinder ($b/d=2$).
1. line: Contribution from velocity square term in Bernoulli's equation.
2. line: Contribution from second order potential.
3. line: Total value.

Here, $T_{ii}^c A_i^2$ is the horizontal drift force on the ship in regular sinusoidal waves of wave amplitude A_i and circular frequency ω_i. Further, ϵ_i are random phase angles (see eqn. (3)). The drift force may be calculated by strip theory. This means the ship is divided into a finite number of strips and the flow around each cross-section is considered independent of each other. When the first order motions of the total ship have been calculated, the drift force can be obtained by either Maruo's beam sea formula (Maruo 1960), or the method presented earlier. Results from comparisons between different methods have been presented by Faltinsen and Løken (1978 b).

The mean horizontal drift and the slowly varying response y_G of the centre of gravity of the moored ship can be obtained from the dynamic equation of motion.

$$\{M+A_{22}(0)\}\frac{d^2y_G}{dt^2}+B_{22}\frac{dy_G}{dt}$$

$$+\frac{\rho}{2}\int_L dxC_D(x)T(x)\left|\frac{dy_G}{dt}-u_c\right|\left(\frac{dy_G}{dt}-u_c\right) \tag{15}$$

$$+\frac{\rho_a}{2}\sum_{i=1}^{1}C_D{}^i\,A_w{}^i\left|\frac{dy_G}{dt}-u_w\right|\left(\frac{dy_G}{dt}-u_w\right)+f(y_G)$$

$$=\sum_{i=1}^{N}\sum_{j=1}^{N}A_iA_jT_{ii}{}^c\cos\left((\omega_j-\omega_i)t-(\epsilon_j-\epsilon_i)\right)$$

We have assumed the wind and current are in the beam direction and the ship has fore and aft symmetry. We may then neglect the effect from yaw motion in a stable system. Further, M is the mass of the ship and $A_{22}(0)$ is the zero-frequency added mass in sway of the ship. B_{22} is a linear damping term due to the wave generation which is likely to be small. It will be dominated by the viscous damping term. The viscous term due to water motion is calculated by a strip theory approach. Reliable information about the sectional drag coefficients, $C_D(x)$ in eqn. (15), is difficult to obtain. They are expected to depend on Reynold's number, Keulegan–Carpenter number and the roughness characteristics of the ship (Sarpkaya 1976). The strip theory approach does not take into account possible large influence of vortex shedding around the ship's ends. The other quantities in the water viscous damping term are the length between perpendiculars L, the sectional drafts $T(x)$ and the water current velocity u_c. The formulation of the viscous drag term can be questioned because we started out with a potential flow formulation, and it is not clear how to properly incorporate the viscous effects. However, our formulation is often used in the literature. The approach presented here does not take into account interaction between the current and the wave field. The viscous term due to air flow is calculated by dividing the superstructure into a number of parts. On each part we associate a drag coefficient $C_D{}^i$. Further, $A_w{}^i$ is the projection of part number i's surface on the centre plane of the ship, ρ_a is the mass density of the air and u_w is the wind velocity. The last term on the left hand side is the effect from the mooring lines. This may be obtained from the mooring line characteristics. The time-dependent part may be approximated by a linear term Ky_G for small amplitudes of oscillations. In a real case, it may not be possible to linearize the effect of the mooring lines. Sometimes a cubic approximation is used, leading to a Duffing equation. Based on linear theory, the natural circular frequency of the sway oscillation will be

$$\omega_N=\sqrt{\left(\frac{K}{M+A_{22}(0)}\right)} \tag{16}$$

Due to small damping in the system, the response will be sharply peaked in the vicinity of ω_N and the response will be very sensitive to variations in excitation periods

around the natural period. This necessitates great care in the selection of number of wave components N (see eqn. (3)). From eqn. (15) and the discussion that followed eqn. (3), the lowest frequency component in the exciting force part of eqn. (15) is $(\omega_{max}-\omega_{min})/N$. Number of wave components can now be determined by requiring that $(\omega_{max}-\omega_{min})/N$ is a certain small fraction of ω_N.

Equation (15) can be solved by a numerical timestep procedure. It should be kept in mind that the damping is quite small. This necessitates quite a long simulation period before transient effects have died out. When the motions are determined, it is straightforward to obtain the resulting loads in the anchor-lines.

The slow drift excitation term (14) and the damping term are equally important in the calculation of the response. The inaccuracy in the determination of the viscous damping term is not expected to be better than the inaccuracy in approximating the slow drift excitation term (12) by eqn. (14). Therefore, the use of the more exact formula for the slow drift excitation does not necessarily lead to a more correct prediction of the resulting loads in the mooring lines.

The procedure described above applies for beam sea irregular long-crested waves in infinite water depth. One may be tempted to generalize the procedure to other wave, current and wind headings, finite water depth and other types of structures. In the general case, the coupled effect of yaw and surge has to be accounted for. The slow drift excitation force in irregular longcrested waves in surge ($m=1$), in sway ($m=2$) and the slow drift excitation moment in yaw ($m=6$) may then be written as

$$F_H^m = \sum_{i=1}^{N}\sum_{j=1}^{N} A_i A_j T_{ii}^m \cos((\omega_j-\omega_i)t-(\epsilon_j-\epsilon_i)) \tag{17}$$

Here, $T_{ii}^m A_i^2$ with $m=1, 2, 6$ is, respectively, the slow drift excitation force in surge and sway and the slow drift excitation moment in yaw on the structure in regular sinusoidal waves of amplitude A_i, circular frequency ω_i and the particular wave propagation direction one is studying. For many types of structures, one may use the general method of Faltinsen and Michelsen (1974) to calculate $T_{ii}^m A_i^2$. The method is based on potential theory and a three-dimensional source technique is used to find the first order potential. Finite water depth is assumed. We would like to point out some of the restrictions of the method. For instance the method is not accepted as valid in steep waves that are breaking or close to breaking. For small volume structures, like semisubmersibles, the viscous effects may be an important part of the drift force. This is not incorporated in the method. Further, for shallow water with small clearance between the bottom and the seafloor, and for a structure where the top of the structure is close to the free surface, there have been difficulties in applying the method. The physical reasons are strong nonlinearities in the flow.

Other methods to calculate mean drift forces and moments are due to Maruo (1960), Gerritsma and Beukelman (1972), Maruo (1957), Newman (1967), Faltinsen and Løken (1978 a), Salvesen (1974), Kaplan and Sargent (1976), Kim and Chou (1973), Pinkster and van Oortmerssen (1977), Ohkusu (1976), Huse (1976), Pijfers and Brink (1977) and Longuet-Higgins (1977). Some of these methods are discussed in detail in Faltinsen and Løken (1978 b), where the limitations and applicabilities of the methods are stressed. In principle it should be possible to generalize eqn. (12) to shortcrested irregular sea. The major difficulty will be in a good estimate of the directional spectra.

5. Conclusions

A procedure to calculate slow drift excitation forces on an infinitely long horizontal cylinder in irregular beam sea waves is presented. The numerical results seem to indicate

(*a*) The contribution from the second order potential to the slow drift excitation forces is small;

(*b*) Calculations based on the velocity square term in Bernoulli's equation can give completely wrong answers;

(*c*) Newman's approximative method is a practical way to calculate horizontal slow drift excitation force on a ship in irregular beam sea waves.

It is suggested that Newman's method may be used to calculate slow drift excitation forces and moment on a large-volume structure in shortcrested irregular waves of any mean wave direction.

Acknowledgment

This report is a part of a research project financially supported by Det norske Veritas and the Royal Norwegian Council for Scientific and Industrial Research (NTNF).

References

Faltinsen, O. (1975). Drift forces on a ship in regular waves, Det norske Veritas Rep. No. 75-4-S.

Faltinsen, O., and Michelsen, F. C. (1974). Motions of large structures in waves at zero Froud numbers. *Proceedings of the International Symposium on Dynamics of Marine Vehicles and Structures in Waves*, London.

Faltinsen, O., and Løken, A. E. (1978 a). Drift forces and slowly varying horizontal forces on a ship in waves. *Proceedings of the Symposium on Applied Mathematics.* (Dedicated to the late Professor Dr. R. Timman), Delft, January 1978; (1978 b). Drift forces and slowly varying forces on ships and offshore structures in waves. Norwegian Maritime Research.

Gerritsma, J., and Beukelman, W. (1972). Analysis of the resistance increase in waves of a fast cargo ship, Nederlands Ship Research Centre TNO, Report No. 169.S.

Houmb, O. G., and Overvik, T. (1976). Parameterization of wave spectra and long term joint distribution of wave height and period. *Proceedings of Behavior of Offshore Structure* '76, Trondheim.

Hsu, F. H., and Blenkarn, K. A. (1970). Analysis of peak mooring forces caused by slow vessel drift oscillations in random seas, Offshore Technology Conference, Houston, paper 1159.

Huse, E. (1976). Wave induced mean force on platforms in direction to wave propagation. *Proc. Interocean.*

Kaplan, P., and Sargent, T. P. (1976). Motions of offshore structures as influenced by mooring and positioning systems, *Proceedings of Behavior of Offshore Structure* '76, Trondheim.

Kim, C. H., and Chou, F. (1973). Prediction of drifting force and moment on an ocean platform floating in oblique waves. *Int. Shipbuilding Progr.*, **20**, p. 388.

Longuet-Higgins, F. R. (1977). The mean forces exerted by waves on floating or submerged bodies with applications to sand bars and wave power machines, *Proc. R. Soc.* (*A*), **352**, p. 463.

Maruo, H. (1960). The drift of a body floating on waves, *J. Ship Res.*, December **4**, 1; (1967). The excess resistance of ship in rough sea, *Int. Shipbuilding Progr.*, **4**, p. 337.

NEWMAN, J. N. (1967). The drift force and moment on ships in waves, *J. Ship Res.*, **11**, p. 51; (1974). Second order, slowly varying forces on vessels in irregular waves, *Proceedings of the International Symposium on Dynamics of Marine Vehicles and Structures in Waves*, London.

OHKUSU, M. (1976). Ship motions in vicinity of a structure, *Proceedings of Behavior of Offshore Structure* '76, Trondheim.

PIJFERS, J. G. L., and BRINK, A. W. (1977). Calculated drift forces of two semisubmersible platform types in regular and irregular waves, Offshore Technology Conference, Houston, paper 2977.

PINKSTER, J. A., and VAN OORTMERSSEN, G. (1977). Computation of the first and second order wave forces on oscillating bodies in regular waves, *Proceedings of the 2nd International Conference on Numerical Ship Hydrodynamics*, Berkeley.

REMERY, G. F. M., and HERMANS, A. J. (1971). The slow drift oscillations of a moored object in random seas, Offshore Technology Conference, Houston.

SALVESEN, N. (1974). Second order steady-state forces and moments on surface ships in oblique regular waves, *Proceedings of the International Symposium on Dynamics of Marine Vehicles and Structures in Waves*, London.

SARPKAYA, T. (1976). Vortex shedding and resistance in harmonic flow about smooth and rough cylinders, *Proceedings of Behavior of Offshore Structure* '76, Trondheim.